Received 25 June 2020; revised 21 July 2020; accepted 23 July 2020. Date of publication 4 September 2020; date of current version 29 September 2020.

Digital Object Identifier 10.1109/OJAP.2020.3021802

A Water-Based Huygens Dielectric Resonator Antenna

RASMUS E. JACOBSEN [1] (Graduate Student Member, IEEE), ANDREI V. LAVRINENKO [1], AND SAMEL ARSLANAGIĆ [2] (Senior Member, IEEE)

[1]Department of Photonics Engineering, Technical University of Denmark, 2800 Kongens Lyngby, Denmark

[2]Department of Electrical Engineering, Technical University of Denmark, 2800 Kongens Lyngby, Denmark

CORRESPONDING AUTHOR: R. E. JACOBSEN (e-mail: rajac@fotonik.dtu.dk)

ABSTRACT With its high-permittivity in the microwave frequency range, water has the potential as an alternative, inexpensive, bio-friendly and abundant material for many microwave applications such as dielectric resonator antennas and tunable metamaterials. Huygens antennas, composed of single-element structures supporting a special combination of electric and magnetic modes, provide an alternative route for compact and directive antennas. In this work, we investigate a subwavelength water-based Huygens dielectric resonator antenna with strongly excited electric and magnetic dipoles at around 350 MHz. Our antenna leads to the directivity of 6 and a radiation front-to-back ratio of 40.3 dB. Additionally, good matching to the feed-line and the surrounding free space were achieved with a reflection coefficient of −38.3 dB and a total efficiency of 57.8 %. The antenna was fabricated and characterized with excellent agreement between the measurements and the numerical results. Furthermore, several means of tuning the antenna were tested numerically and experimentally. We believe that the proposed water-based Huygens dielectric resonator antenna may serve as an easy–to–fabricate and cheap alternative for the VHF and low end of the UHF bands.

INDEX TERMS Dielectric resonator antenna, reconfigurable antennas, water.

I. INTRODUCTION

OVER several decades, dielectric resonator antennas (DRAs) have been of great interest as compact alternatives to traditional dipole and waveguide antennas [1]. Many designs have been proposed demonstrating different attributes such as low-profile, large bandwidth, frequency-tunability and phase-steering capabilities. Generally, DRAs rely on electric and magnetic modes supported in expensive high-permittivity ceramic structures. Alternatively, water-filled cavities exploiting water's relatively high permittivity in the microwave frequency range can be used instead [2]. Water holds great potential as an abundant, inexpensive and bio-friendly material for tunable antennas [3]–[5], as well as inclusions in metamaterials (MMs) and metasurfaces (MSs) [6]–[11].

Various liquid-based antennas have been demonstrated with some relying on water's high real and low imaginary parts of permittivity, whereas other use conductive liquids [3]–[5], [12]. In general, many of these antennas operate in the VHF and UHF bands due to the decreasing (increasing) real part of water's permittivity at higher frequencies. The working principle of water-based DRAs relies on resonant electric (TM) and magnetic (TE) modes in water-filled cavities. These modes are the natural eigenmodes belonging to the dielectric cavity, and they can be excited by sources placed outside and inside the cavity. In general, a single cavity has multiple modes spread-out in narrow bands of frequencies across the spectrum. In [5], we demonstrated an electrically small water-based hemispherical DRA with such characteristics. The water provided an excellent way to place an adjustable metallic monopole antenna inside the cavity without the issues of air gaps between the dielectric and the monopole antenna. Furthermore, the water-based DRA could be tuned by changing the water-temperature and/or the water-volume in the cavity.

This work is licensed under a Creative Commons Attribution 4.0 License. For more information, see https://creativecommons.org/licenses/by/4.0/

In antenna configurations, the dipole modes are the most broadly used, which by their nature have low directivity. Higher-order modes can also be exploited for high-directivity antennas, but such higher-order modes require larger dielectric structures, have very small bandwidths and are more sensitive to losses [1]. Another way to increase the directivity in a compact single-element configuration is to combine magnetic and electric modes [13]–[15], and such antennas are often referred to as Huygens antennas. Furthermore, when the fundamental dipole modes are combined in dielectric structures, Kerker's condition may be satisfied [16]–[17], which is also of great interest in MMs and MSs. Additionally, dipoles and higher-order modes can also be combined to increase the directivity even further [17]–[18]. Kerker's condition is satisfied in many types of dielectric structures, including dielectric spheres and cylinders [19]–[20]. However, the dipole modes are often weakly excited resulting in very low scattering. Designing structures exhibiting strongly excited magnetic and electric modes with the right integration of their magnitudes and phases is not a simple task. Combining an electric and magnetic dipole will increase the directivity in one direction to twice of that of a single dipole, while in the opposite direction, the directivity is greatly minimized. Several Huygens antenna designs have already been demonstrated [13]–[14], [18], but thus far no water-based Huygens DRAs have been proposed.

The purpose of the present work is to investigate a simple subwavelength water-based Huygens DRA. The antenna consists of a short monopole antenna fed against a large ground conducting plane and encapsulated by a rectangular cuboid-shaped cavity filled with distilled water. The DRA is designed with overlapping fundamental electric and magnetic dipole modes at around 350 MHz. The final design has a directivity of 6 and a front-to-back ratio (FBR) of 40.3 dB. Furthermore, our antenna is well matched to both its feed-line and the surrounding free space with a reflection coefficient of -38.3 dB and a total efficiency of 57.8 %. The size of the antenna is $a \approx 147$ mm $\approx \lambda_0/6$ (sometimes provided as $k_0 a \approx 1.08$), where λ_0 ($k_0 = 2\pi/\lambda_0$) is the free-space wavelength (wave number). A prototype of the antenna is fabricated with excellent agreement between numerical results and measurements. In addition, we demonstrate and discuss several ways of tuning the antenna. We believe that the simple and cheap antenna serve as an easy–to–fabricate and cheap alternative for the VHF and low end of the UHF bands.

Throughout this article, the time-factor $\exp(j\omega t)$, with ω being the angular frequency and t being the time, is assumed and suppressed.

II. ANTENNA CONFIGURATION AND PARAMETERS

A sketch of the water-based Huygens DRA is shown in Fig. 1. It consists of a rectangular cuboid-shaped Rohacell 51 HF cavity attached to a ground conducting plane and filled with distilled water. The Rohacell 51 HF materials has a measured relative permittivity of 1.075 [9]. A Cartesian

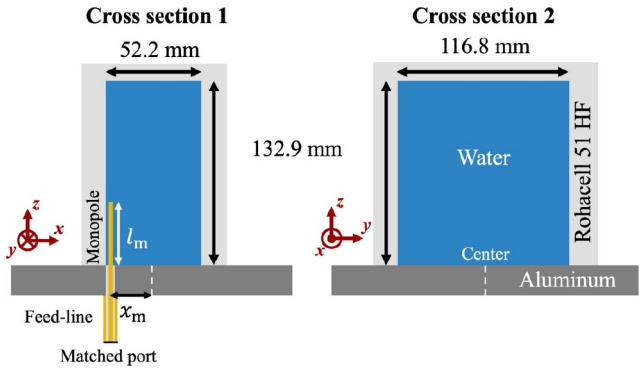

FIGURE 1. A sketch of the water-based Huygens DRA.

coordinate system is introduced as shown in Fig. 1 with the associated spherical angular coordinates (θ, ϕ). A short monopole is inserted into the cavity as shown in Fig. 1. The feed line is a coaxial transmission line with the inner and outer diameter of 1.28 mm and 4.1 mm, respectively, and a dielectric material with the relative permittivity of 2.1. The characteristic impedance of the feed line is 48.15 Ω. The diameter and the length of the monopole is 1.6 mm and l_m, respectively. The monopole is displaced by $x = -x_m$ from the center of the Huygens DRA to excite the magnetic mode. The Huygens DRA is designed for 350 MHz operation with a water temperature of 20°C. The final design with the highest total efficiency (η_{tot}) and FBR were determined through a parametric study. In a previous work, we investigated a water-based hemispherical DRA, which exhibited both magnetic and electric dipole resonances, however, with the latter being at higher frequencies [5]. A cubic DRA has similar behavior, and to shift the electric resonance to lower frequencies, we simply extend the dielectric along the y- and z-axis until we obtain the wanted properties of the antenna. The cavity size and the values of x_m and l_m are listed in Table 1 for the final antenna design.

The *xz*- and *xy*-planes correspond to the E- and H-planes of the antenna, respectively. The Debye model is used to describe the permittivity of distilled water inside the cavity [2], and at 350 MHz and 20°C, the relative permittivity is $\varepsilon_{r,water}$ (350 MHz, 20°C) $= 80.2 - j1.6$. A model of the Huygens DRA is built in COMSOL Multiphysics 5.4 used for all numerical calculations [21]. The COMSOL model consists of the Huygens DRA enclosed by a hemisphere of free space and with a Perfect Electric Conductor (PEC) plane as the ground. The Huygens DRA is simulated without the Rohacell 51 HF material as its low permittivity minimally affects the antenna response. An outer layer of PML is attached to the free-space hemisphere and a matched port is placed on the bottom of the feed line. A symmetry plane was employed at $y = 0$ to half the model size and a convergence test was conducted leading to total of 1,283,616 Number of Degrees of Freedom solved for in the final model.

We use different well-known antenna parameters in this article, such as total efficiency (including the mismatch loss)

TABLE 1. Simulated water-based Huygens antenna parameters.

Parameter	Value
Cavity size [mm^3]	116.8×52.2×132.9
l_{m} [mm]	27.2
x_{m} [mm]	24
f [MHz]	351.6
$G_{\mathrm{realized,max}}$ [dBi]	5.42
D_{max}	6
η_{tot}	57.8 %
η_{rad}	57.8 %
$\lvert S_{11}\rvert$ [dB]	–38.3
Z_{A} [Ω]	$47.27 + j0.77$
$\mathrm{FBW}_{10\mathrm{dB}}$	4.0 %
$\mathrm{FBR}_{\mathrm{max}}$ [dB]	40.3
$k_0 a$ [rad]	1.08
$\varepsilon_{\mathrm{r,water}}$(350 MHz, 20 °C)	$80.2 - j1.6$

η_{tot}, radiation efficiency η_{rad}, reflection coefficient S_{11} etc., and we refer to [5] or [22] for more information about these parameters. Throughout the paper we use the front-to-back ratio (FBR) to evaluate how well the radiated power is concentrated in one direction. The FBR is defined as

$$\mathrm{FBR} = D_{+x}/D_{-x}, \tag{1}$$

where $D_{\pm x}$ is the directivityin the $\pm x$-direction (in angular coordinates: $(\theta, \phi)_{+x} = (90°, 0°)$ and $(\theta, \phi)_{-x} = (90°, 180°)$).

III. NUMERICAL AND EXPERIMENTAL RESULTS

A. ANTENNA CHARACTERIZATION

The final results are summarized in Table 1. We present η_{tot} and η_{rad} as functions of frequency in Fig. 2(a). The magnitude of S_{11} as function of frequency is shown in Fig. 2(b). Around 350 MHz the efficiencies are high, and S_{11} is low. At 351.6 MHz, where FBR is maximum (see Fig. 4(a)), the S_{11} drops to −38.3 dB indicating excellent matching of the antenna to the feed-line. The antenna input impedance Z_A is calculated using S_{11}, and its real and imaginary parts are shown in Fig. 2(c) as functions of frequency. At 351.6 MHz, $Z_{\mathrm{A}} = 47.27 + j0.77\Omega$. η_{tot} is modest and is 57.8 % as the water absorbs 42.2 % of the input power. The absorbed power was calculated in COMSOL by integrating the power loss density over the volume of water.

The peak in η_{tot} comes from the modes excited in the water-filled cavity. From Fig. 2, we would conclude that a single resonant mode is excited around 350 MHz. However, inspecting the near fields of the antenna in both the xz- and xy-plane, which are shown in Fig. 3, we observe two dipoles being excited. The displacement of the monopole along the x-axis inside the water cavity renders an asymmetric field distribution, and in the xz-plane in Fig. 3(a), we see that the electric field (arrows) forms a half-loop

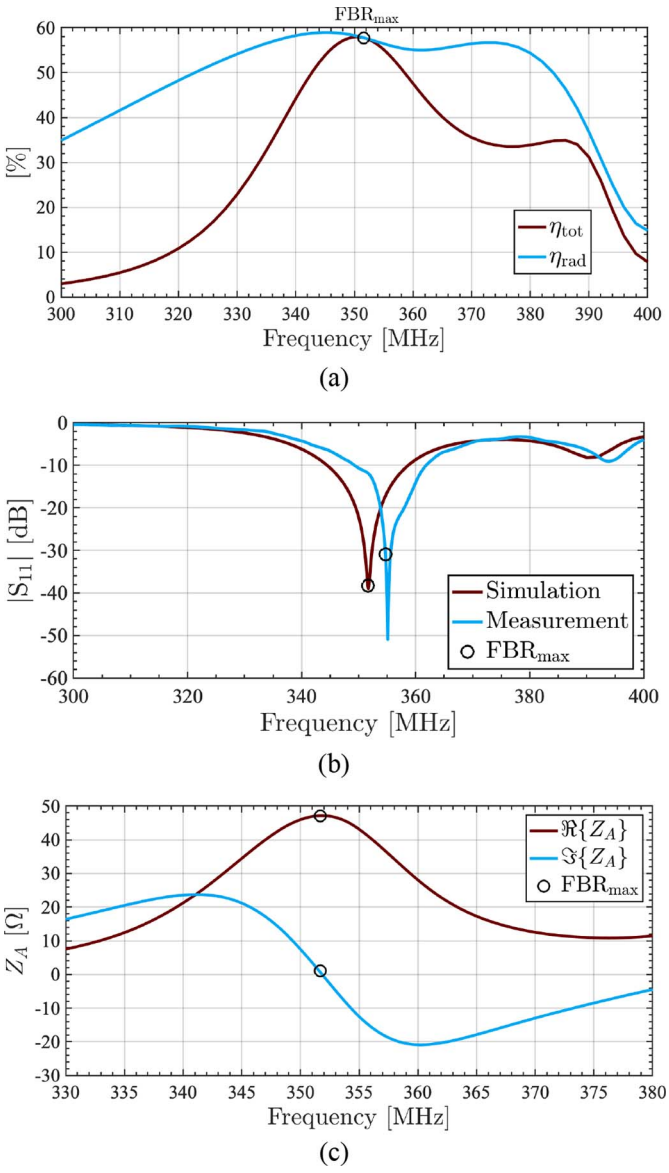

FIGURE 2. The simulated (a) total efficiency (η_{tot}) and radiation efficiency (η_{rad}) and (b) the reflection coefficient (S_{11}) as functions of frequency. The circles indicate the location of maximum FBR. In (b), S_{11} is given in logarithmic scale, and the measured S_{11} is included. The antenna input impedance Z_{A} is shown as a function of frequency in (c).

with an enhanced magnetic field intensity (colors) near the ground plane inside the water. This is identified as a magnetic dipole mode (TE_{111}). If we turn our attention to the xy-plane in Fig. 3(b), we find an alternated field distribution: the magnetic field (arrows) forms a loop with an enhanced electric field intensity (colors), i.e., an electric dipole (TM_{011}). In our previous work on water-based antennas, such strong dipole modes were also excited, but at different frequencies [5]. In the present configuration, the dipoles are excited at the same frequency. The outcome of the double dipole excitation can also be observed in the far-field, see Fig. 4(a), where the directivity pattern has the cardioid shape. The directivity in the $-x$-direction is greatly

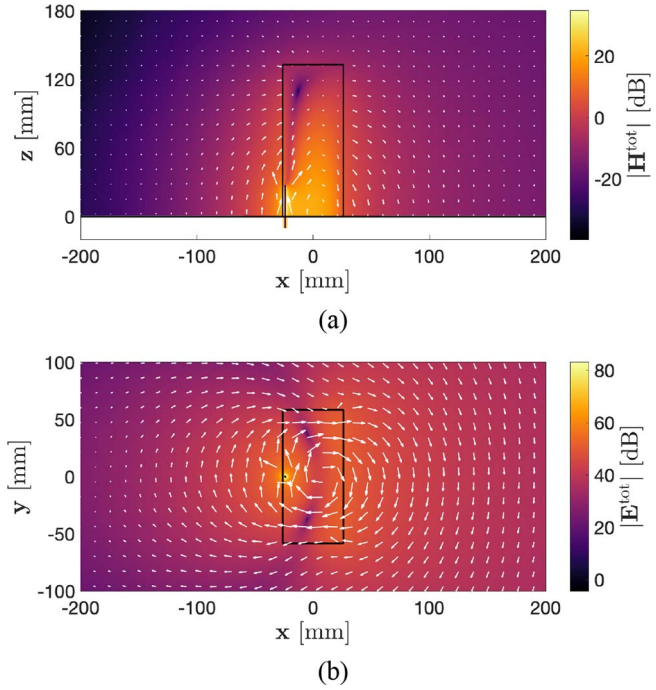

FIGURE 3. (a) The total magnetic (electric) field intensity, H^{tot} (E^{tot}), shown as colors (arrows) in the *xz*-plane. (b) E^{tot} (H^{tot}) shown as colors (arrows) in the *xy*-plane. Both colors and arrows are in logarithmic scale. Frequency is 351.6 MHz. There is no radiation in the negative *z*-direction because of the ground plane.

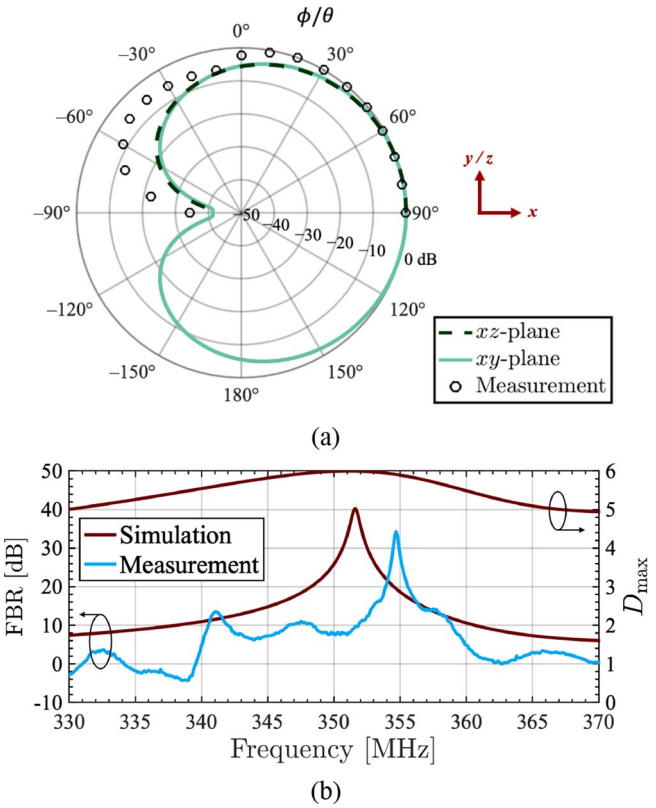

FIGURE 4. (a) Simulated radiation pattern shown by the normalized directivity in the *xz*- and *xy*-planes at the frequency of 351.6 MHz. The black circles show the measured normalized $|S_{21}|$ in the *xz*-plane at the frequency of 354.7 MHz. The simulated directivity and measured S_{21} are normalized with their maximum values and given in logarithmic scale for easier comparison. (b) Simulated and measured front-to-back ratio (FBR) in logarithmic scale, as well as the maximum directivity (D_{max}), as functions of frequency.

reduced, whereas the maximum in the $+x$-direction is still maintained. Such behavior is highlighted in Fig. 4(b) with the FBR shown as a function of frequency. At 351.6 MHz, the FBR has the remarkable peak value of 40.3 dB. The maximum directivity $D_{\max} = D_{+x}$ as a function of frequency is included in Fig. 4(b). At 351.6 MHz, $D_{\max} = 6$, which is expected for ground-supported Huygens antennas [15]: a single dipole antenna has a directivity of 1.5, and with two dipoles and a ground plane, the directivity is increased by a factor of 4. Furthermore, the maximum realized gain is $G_{\text{realized,max}} = 5.42$ dBi, which is 0.65 dB higher than that of a matched and lossless monopole antenna.

The antenna was fabricated at the local workshop, and a photograph is shown in Fig. 5(a). The antenna was made by hollowing out the cavity in a Rohacell 51 HF block, which was then glued on to a circular aluminum plate of 1 m in diameter. Holes for insertion of the monopole antenna and distilled water were drilled in the aluminum plate. A sketch of the measurement setup is shown in Fig. 5(b). The antenna was mounted on a tripod with a rotating joint such that the antenna could be rotated θ' as shown in Fig. 5(b). In this way, the radiation pattern was recorded using a simple dipole antenna designed for 350 MHz operation and positioned 3.3 m away. Accordingly to the definition of the far-field distance, if we use the ground plane as the largest dimension ($d = 1$ m is the size of the ground plane), we get $d_{\text{ff}} > 2d^2/\lambda_0 \approx 2.3$ m and thus fulfill the far-field condition. For measurement angles $\theta' = [90°, 0°[$, the antenna was rotated 180° in the *xy*-plane. The reflection (S_{11}) and transmission coefficients ($S_{21}(\theta')$) were measured with an Anritsu MS2024B vector network analyzer calibrated for 50 Ohm matching. The measured S_{11} is shown in Fig. 2(b) and the measured FBR is included in Fig. 4(b), which is calculated as $S_{21}(\theta' = 90°)/S_{21}(\theta' = -90°)$. The measured FBR is maximal at 354.7 MHz with a measured S_{11} of -30.9 dB showing nice agreement with the numerical predictions. The small mismatch of 3.1 MHz in frequency between experimental and numerical results can be explained by a small difference in temperature and/or water filling in the cavity. The normalized measured $S_{21}(\theta')$ in the *xz*-plane is included in Fig. 4(a), and is in good agreement with the numerical results.

By default, the antenna bandwidth is characterized by its 3-dB fractional matched voltage standing wave ratio bandwidth $\text{FBW}_{3\text{dB}}$ [22]. However, due to the second resonance around 390 MHz, this is quite large (19.7 %). Therefore, it is more convenient in this case to use the 10-dB fractional matched voltage standing wave ratio bandwidth $\text{FBW}_{10\text{dB}}$, which is 4.0 %. According to [23], the quality factor Q is given by $Q = 2/3\text{FBW}_{10\text{dB}}$, which in the case of our Huygens DRA gives around 17. In the absence of water, one is left with the monopole antenna alone, which resonates

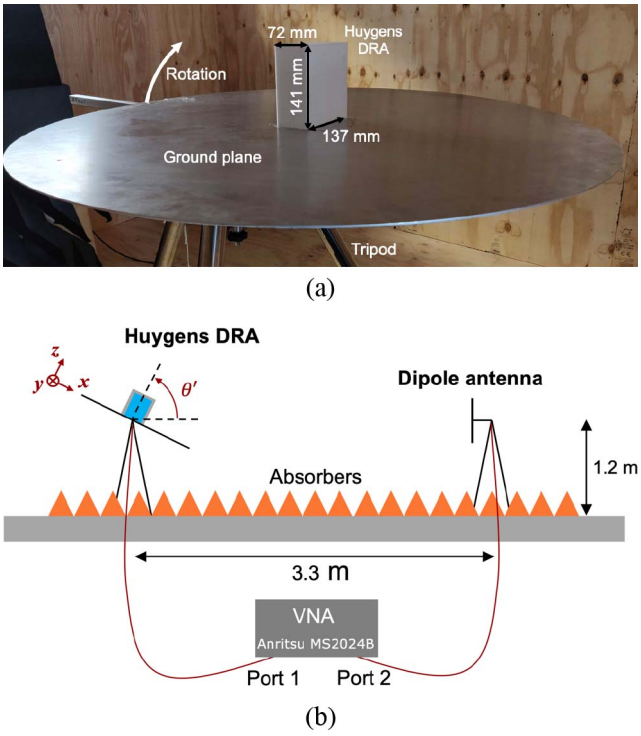

FIGURE 5. (a) Photograph of the fabricated antenna mounted the tripod with the rotatable joint and (b) sketch of the measurement setup.

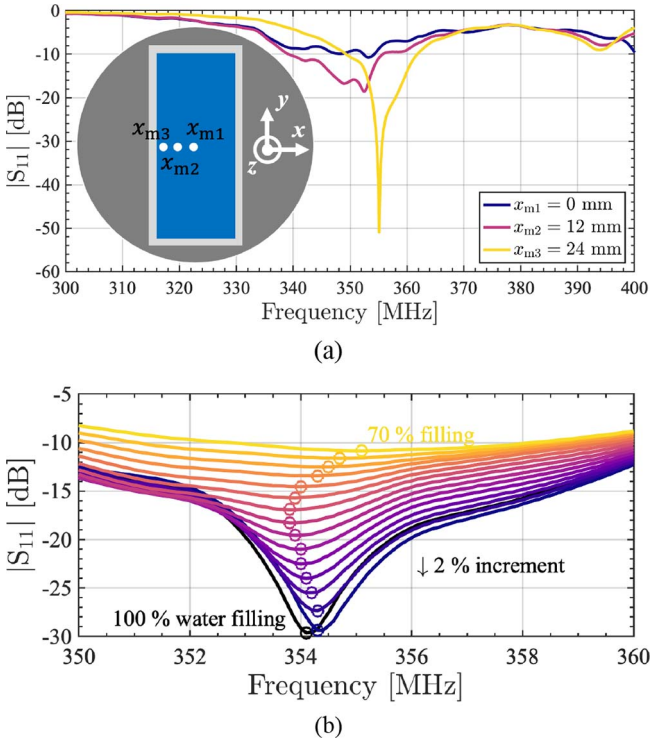

FIGURE 6. Measured S_{11} in logarithmic scale as a function of frequency for different positions of the monopole antenna ($x = -x_m$) in (a) and for variation of the water content in (b). A sketch of the antenna cross section with the monopole antenna positions is included as an inset in (a). The circles in (b) show the minimum of each graph.

at a higher frequency (around 2.8 GHz) with an associated quality factor of around 7 [22]. From Fig. 4(b), we see that the high FBR is narrow-banded. Obviously, this is coming from the tight overlap of the resonant dipole modes. The FBR_{10dB} bandwidth is 6.5 %.

B. TUNABILITIES AND SENSITIVITIES

Water-based antennas have multiple tuning parameters, and in this work, we have tested variations of the position of the monopole, water content in the cavity and temperature of water.

In total three holes were drilled for the insertion of the monopole, and the measured S_{11} for each of them is shown in Fig. 6(a). For the alternative monopole positions, $x_m = 0$ and $x_m = 12$ mm, we find several minima spread out over their spectra, each representing different mode excitations. None of these modes produce reflection coefficients below -20 dB, and their radiation patterns are different from that shown in Fig. 4(a). In Fig. 7(a), we have included the simulated realized gain $G_{realized}$ as a function of θ in the xz-plane as the monopole antenna position is shifted along the x-axis. The inset shows the angle of each minima (null) in $G_{realized}$, θ_{min}, as a function of x_m. At $x_m = 0$, the radiation pattern is symmetric with the null being at 0°. As x_m increases, the null shifts towards the negative angles, and at $x_m = 24$ mm, the null reaches $-90°$. These results demonstrate the beam-steering capabilities of the antenna with a simple re-positioning of the monopole antenna. Similar study was conducted in [3] showing same tendency. Additionally, further beam-steering should be possible by also displacing the monopole antenna in the y-direction.

Another way to tune the water-based antennas is to simply remove/add water (see, e.g., [4]–[5]). Presently, we stepwise remove 2 % of the water from the cavity, until 70 % water is left, measuring S_{11} after each water extraction. The result is shown in Fig. 6(b) and an aggravation of S_{11} is observed as the water content in the cavity is reduced (please note that the measurements in Fig. 6(a) and Fig. 6(b) were carried out at days with different temperatures causing the minor differences in the measured S_{11}). A similar study has previously been conducted for another water-based DRA, where a linear blue-shift was observed [5]. However, we do not observe similar tendency for the present design. As the water content is reduced, the radiation in the xz-plane becomes less directive and more omnidirectional as shown in Fig. 7(b) by $G_{realized}$ as a function of θ in the xz-plane. The antenna has the response shown in Fig. 6(b) and Fig. 7(b) as long as it is kept in level. If any deviations in angle theta in positioning of the AUT happens, then water no more can be accurately described as a cuboid dielectric. This is quite complicated behavior as the resonance frequency and radiation pattern will change for different theta angles. This can be a subject of further analysis. Seen from another perspective, this presents a great way to, e.g., completely level the antenna or to check if the cavity is 100 % filled. In addition,

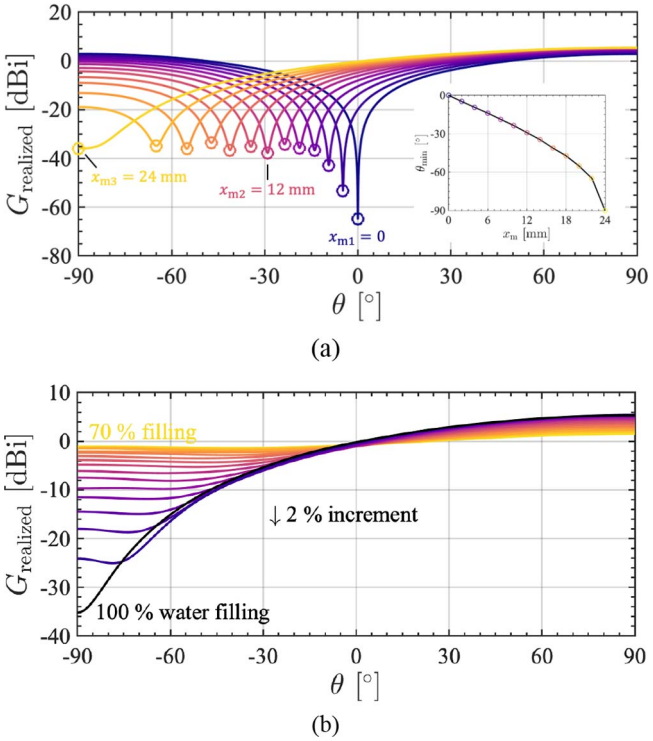

FIGURE 7. Simulated realized gain ($G_{realized}$) as a function of θ in the *xz*-plane for (a) different positions of the monopole antenna (x_m) and (b) for variation of the water content. Frequency is 351.6 MHz and $G_{realized}$ is shown in logarithmic scale. The circles in (a) show the minima (null) of each graph and their angles, θ_{min}, are plotted as a function of x_m in the inset.

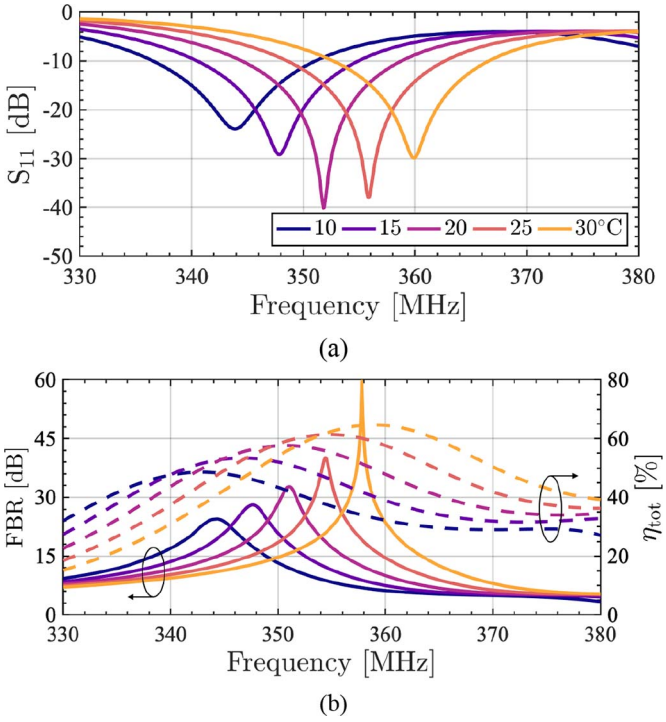

FIGURE 8. Simulated temperature variations from 10°C to 30°C. (a) S_{11} and (b) FBR and η_{tot} shown as functions of frequency. S_{11} and FBR are given in logarithmic scale.

the antenna should be sensitive to vibrations. We have not made such comprehensive studies this work.

Water's complex permittivity is temperature-dependent, and it decreases with increasing temperature. This property can also be exploited to tune the response of water-based antennas as well as other types of water-based devices [4]. Presently, we simulate minor variations of water's temperature, and in Fig. 8, S_{11}, FBR and η_{tot} are shown as functions of frequency. As the temperature increases from 10°C to 30°C, the response is blue-shifted by approximately 16 MHz. Furthermore, both η_{tot} and FBR improve due to the lower losses, whereas the matching, indicated by the minimum of S_{11}, is optimum around 20 °C. Still, the minimum of S_{11} stays below −20 dB at all simulated temperatures.

The results in Fig. 6, 7 and 8 demonstrate the antenna's tunabilities, but it can also be viewed as its sensitivities to fabrication variations and defects as well as changes in the local environment. The antenna has other tunabilities/sensitivities as, e.g., the impurities in the water, which we did not test in this work.

C. FURTHER DISCUSSIONS

The antenna's electrical size is $k_0a \approx 1.08$ ($\lambda_0/6$), and therefore, not categorized as being electrically small, which requires $k_0a \leq 0.5$ for ground-supported antennas, see, e.g., [5] and [24]. Still, the antenna is several times smaller than many other DRAs [1], [4], and the modest efficiency is higher than, e.g., a directive subwavelength DRA composed of an expensive low-loss ceramic material [18]. In our case, we have a simple and cheap antenna. Furthermore, the antenna is tunable and self-matched to a 50 Ohm transmission line, and thus, no matching components are needed. The directivity is twice that of traditional single-unit DRAs in which only magnetic or electric modes are excited [1]. Due to the losses in water and the compact design, the efficiency is modest compared to other DRAs.

In Fig. 2, we find a second mode being excited around 385 MHz. The mode is weakly excited, which explains the low efficiency. Inspecting the field distribution and radiation pattern (not shown in the manuscript), we conclude that it is another magnetic mode.

IV. SUMMARY AND CONCLUSION

A simple water-based Huygens DRA consisting of a short monopole antenna fed against a large conducting ground plane and encapsulated by a rectangular cuboid-shaped cavity filled with water was investigated. With strongly excited magnetic and electric dipoles, an excellent front-to-back ratio of 40.3 dB was achieved as well as good matching to the feed-line and the surrounding space with a reflection coefficient of −38.3 dB and a total efficiency of 57.8 %. Furthermore, the achieved maximum directivity was 6 in accordance with the expectations. The antenna was fabricated and characterized with the measurements exhibiting

excellent agreement with the numerical results. We demonstrated several ways of tuning the Huygens DRA's response with both numerical and experimental studies.

With its simple and versatile, as well as extremely cheap and bio-friendly design, the Huygens DRA may serve as an alternative antenna for microwave communication systems operating in the VHF and low end of the UHF bands. Additionally, the Rohacell material is not essential for the functionality of the antenna and can therefore be replaced by cheaper and more bio-friendly alternatives to even further minimize the ecological footprint of the device.

ACKNOWLEDGMENT

The authors would like to thank the workshop at the Electromagnetic Systems group of the Technical University of Denmark for fabrication of the antennas.

REFERENCES

[1] A. Petosa and A. Ittipiboon, "Dielectric resonator antennas: A historical review and the current state of the art," *IEEE Antenn. Propag. Mag.*, vol. 52, no. 5, pp. 91–116, Oct. 2010.
[2] W. Ellison, "Permittivity of pure water, at standard atmospheric pressure, over the frequency range 0–25 THz and the temperature range 0–100°C," *J. Phys. Chem. Ref. Data*, vol. 36, pp. 1–18, Feb. 2007.
[3] S. P. Kingsley and S. G. O'Keefe, "Beam steering and monopulse processing of probe-fed dielectric resonator antennas," *IEE Proc. Radar Sonar Navig.*, vol. 146, no. 3, pp. 121–125, Jun. 1999.
[4] E. Motovilova and S. Y. Huang, "A review on reconfigurable liquid dielectric antennas," *Materials*, vol. 13, no. 8, p. 1863, Apr. 2020.
[5] R. E. Jacobsen, A. V. Lavrinenko, and S. Arslanagicì, "Electrically small water-based hemispherical dielectric resonator antenna," *Appl. Sci.*, vol. 9, no. 22, pp. 2076–3417, Nov. 2019
[6] A. Andryieuski, S. M. Kuznetsova, S. V. Zhukovsky, Y. S. Kivshar, and A. V. Lavrinenko, "Water: Promising opportunities for tunable all-dielectric electromagnetic metamaterials," *Sci. Rep.*, vol. 5, Aug. 2015, Art. No. 13535.
[7] M. A. Gorlach, M. Song, A. P. Slobozhanyuk, A. A. Bogdanov, and P. Belov, "Topological transition in coated wire medium," *Phys. Status Solidi RRL*, vol. 10, no. 12, pp. 900–904, Oct. 2016.
[8] X. Yang, D. Zhang, S. Wu, L. Li, K. Cao, and K. Huang, "Reconfigurable all-dielectric metasurface based on tunable chemical systems in aqueous solution," *Sci. Rep.*, vol. 7, p. 3190, Jun. 2017.
[9] R. E. Jacobsen, A. V. Lavrinenko, and S. Arslanagicì, "Water-based metasurfaces for effective switching of microwaves," *IEEE Antennas Wireless Propag. Lett.*, vol. 17, pp. 571–574, 2018.
[10] Y. J. Yoo *et al.*, "Metamaterial absorber for electromagnetic waves in periodic water droplets," *Sci. Rep.*, vol. 5, Sep. 2015, Art. No. 14018.
[11] F. Yang *et al.*, "Ultrabroadband metamaterial absorbers based on ionic liquids," *Appl. Phys. A*, vol. 125, no. 2, pp. 1–9, Feb. 2019.
[12] L. Xing, Y. Huang, Q. Xu, and S. Al Ja'afreh, "Overview of water antenna designs for wireless communications," in *Proc. IEEE 4th Asia–Pac. Conf. Antennas Propag. (APCAP)*, Kuta, Indonesia, 2015, pp. 233–234.
[13] M. C. Tang, B. Zhou, and R. W. Ziolkowski, "Low-profile, electrically small, Huygens source antenna with pattern-reconfigurability that covers the entire azimuthal plane," *IEEE Trans. Antennas Propag.*, vol. 65, no. 3, pp. 1063–1072, Mar. 2017.
[14] M. C. Tang, W. Zhentian, T. Shi, and R. W. Ziolkowski, "Dual-band, linearly polarized, electrically small Huygens dipole antennas," *IEEE Trans. Antennas Propag.*, vol. 67, no. 1, pp. 37–47, Jan. 2019.
[15] R. W. Ziolkowski, "Using Huygens multipole arrays to realize unidirectional needle-like radiation," *Phys. Rev. X*, vol. 7, no. 3, Jul. 2017, Art. no. 031017.
[16] M. Kerker, D.-S. Wang, and C. L. Giles, "Electromagnetic scattering by magnetic spheres," *J. Opt. Soc. Amer.*, vol. 73, no. 6, pp. 765–767, 1983.
[17] R. Alaee, R. Filter, D. Lehr, F. Lederer, and C. Rockstuhl, "A generalized Kerker condition for highly directive nanoantennas," *Opt. Lett.*, vol. 40, no. 11, pp. 2645–2648, 2015.
[18] A. E. Krasnok, D. S. Filonov, C. R. Simovski, Y. S. Kivshar, and P. A. Belov, "Experimental demonstration of superdirective dielectric antenna," *Appl. Phys. Lett.*, vol 104, no. 13, Mar. 2014, Art. no. 133502.
[19] M. Decker *et al.*, "High-efficiency dielectric Huygens' surfaces," *Adv. Opt. Mater.*, vol. 3, no. 6, pp. 813–820, Feb. 2015.
[20] D. Tsarouchis and A. Sihvola, "Light scattering by a dielectric sphere: Perspectives on the Mie resonances," *Appl. Sci.*, vol. 8, no. 2, p. 184, 2018.
[21] (2018). *COMSOL Multiphysics 5.4*. [Online]. Available: https://www.comsol.com/
[22] C. A. Balanis, *Antenna Theory*, 4th ed. Hoboken, NJ, USA: Wiley, 2016, pp. 60–63.
[23] A. D. Yaghjian and S. R. Best, "Impedance, bandwidth, and Q of antennas," *IEEE Trans. Antennas Propag.*, vol. 53, no. 4, pp. 1298–1324, Apr. 2005.
[24] A. Erentok and R. W. Ziolkowski, "Metamaterial-inspired efficient electrically small antennas," *IEEE Trans. Antennas Propag.*, vol. 56, no. 3, pp. 691–707, Mar. 2008.

RASMUS E. JACOBSEN (Graduate Student Member, IEEE) received the M.Sc. degree in electrical engineering from the Technical University of Denmark in 2017, where he is currently pursuing the Doctoral degree with Photonics Engineering and Electrical Engineering Departments.

He was a Visiting Scholar with the Advanced Science Research Center, City University of New York, USA, in the winter of 2020. His current research interests include water-based electromagnetic devices such as metamaterials, antennas, and sensors.

ANDREI V. LAVRINENKO received the M.S., Ph.D., and D.Sci. degrees from the Belarusian State University (BSU), Minsk, Belarus, in 1982, 1989, and 2004, respectively.

He was an Assistant Professor and an Associate Professor with the Department of Physics, BSU, from 1990 to 2004. Since 2004, he has been an Associate Professor with the Department of Photonics Engineering, Technical University of Denmark, Kongens Lyngby, Denmark, where he has been leading the Metamaterials Group since 2008. He has authored five textbooks, ten book chapters, and more than 190 journal papers. His research interests include metamaterials, plasmonics, photonic crystals, quasicrystals and photonic circuits, slow light, and numerical methods in electromagnetics and photonics.

SAMEL ARSLANAGIĆ (Senior Member, IEEE) was born in Sarajevo, Bosnia and Herzegovina, in 1979. He received the M.Sc. and Ph.D. degrees from the Department of Electrical Engineering, Technical University of Denmark (DTU) in 2004 and 2007, respectively.

He was appointed as an Associate Professor in applied electromagnetics with DTU in 2012. He was a Visiting Scholar with the Electromagnetics Laboratory, University of Arizona, USA, in the fall of 2005 and the summer of 2011. He has authored or coauthored more than 30 journal papers, 66 conference papers, four book chapters and three technical reports. His research interests include, in brief, radiation and scattering of electromagnetic waves from complex material structures from radio to optical frequencies, as well as the broad area of electromagnetic education. He received the DTU Student Union's Teacher of the Year Award in 2018 for his teaching in electromagnetics and wireless communication courses.